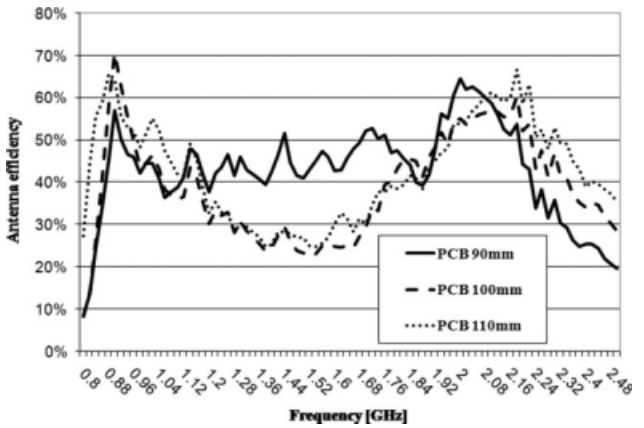

Figure 14 Measured total efficiency of the antenna as a function of the frequency. The measurement system is Satimo which uses 3D pattern integration to calculate total antenna efficiency

PCB larger, the bandwidth increases. At low band, increasing the PCB from 90 to 110 mm, the bandwidth is increased a ratio of 1.6. However, this value is 1.5 at high band. The presented technique is very useful to satisfy the systems of GSM850/GSM900, DCS, PCS, and UMTS.

Finally, various prototypes have been implemented. These prototypes have corroborated the trends of the simulations.

The SAR study is underway and it will be presented in future works.

REFERENCES

1. K. Wong, G. Lee, and T. Chiou, A low-profile planar monopole antenna for multiband operation of mobile handsets, IEEE Trans Antennas Propag 51 (2003).
2. H. Nakano, N. Ikeda, Y. Wu, R. Suzuki, H. Mimaki, and J. Yamauchi, Realization of dual-frequency and wide-band VSWR performances using normal-mode helical and inverted-F antennas, IEEE Trans Antennas Propag 46 (1998), 788–793.
3. J. Jung, H. Choo, and I. Park. Design and performance of small electromagnetically coupled monopole antenna for broadband operation, IET Microwave Antennas Propag 1 (2007).
4. K. Wong, Planar antennas for wireless communications, Wiley series in Microwave and Optical engineering, 2003, pp. 72–126.
5. Patent application WO 2004/025778.
6. S. Risco, Coupled monopole antenna techniques for handset devices, Bachelor Thesis in Electrical Engineering, Universitat Ramon Llull, Barcelona, 2008.
7. J. Anguera, C. Puente, and C. Borja, A procedure to design stacked microstrip patch antennas based on a simple network model, Microw Opt Technol Lett 30 (2001), 149–151.
8. J. Anguera, Fractal and broadband techniques on miniature, multifrequency, and high-directivity microstrip patch antennas, Ph.D. Dissertation, Department of Signal Theory and Communications, Universitat Politècnica de Catalunya, 2003.
9. T.Y. Wu and K.L. Wong, On the impedance bandwidth of a planar inverted-F antenna for mobile handset, Microwave Opt Technol Lett 32 (2002), 249–251.

APERTURE EFFICIENCY ANALYSIS OF REFLECTARRAY ANTENNAS

Ang Yu,[1] Fan Yang,[1] Atef Z. Elsherbeni,[1] John Huang,[2] and Yahya Rahmat-Samii[3]
[1] Department of Electrical Engineering, The University of Mississippi, University, Mississippi 38677; Corresponding author: ayu@olemiss.edu
[2] Retiree from Jet Propulsion Laboratory, California Institute of Technology, Pasadena, California 91109
[3] Department of Electrical Engineering, University of California, Los Angeles, California 90095

Received 26 May 2009

ABSTRACT: *In the design procedure of a reflectarray antenna system, the aperture efficiency needs to be first analyzed to forecast the system performance. This article investigates the effects of the reflectarray configuration parameters on the antenna aperture efficiency. A general approach is introduced to calculate the spillover efficiency of a reflectarray with arbitrarily shaped aperture and feed scheme. Meanwhile, the illumination efficiency of the reflectarray is analyzed with a unified set of equations. On the basis of these derivations, parametric studies are performed to provide design guidelines for optimizing the aperture efficiency of reflectarray antennas.* © 2009 Wiley Periodicals, Inc. Microwave Opt Technol Lett 52: 364–372, 2010; Published online in Wiley InterScience (www.interscience.wiley.com). DOI 10.1002/mop.24949

Key words: *aperture efficiency; illumination efficiency; spillover efficiency; reflectarray*

1. INTRODUCTION

In the last decade, there is an increasing interest in reflectarray antennas, which combines the advantages of both traditional reflector antennas and conventional phased array antennas [1–3]. The element phases are individually controlled to achieve a specific radiation beam, whereas the spatial feeding method eliminates the energy loss and design complexity of a feeding network. Figure 1 shows a general configuration of a reflectarray antenna, which includes an array of scattering elements and a feeding source located above. The array elements are usually located on a planar aperture, which can be a circular, square, or other general shapes. The feeding source can be central positioned or off set depending on specific applications.

Similar to the design of a conventional reflector, the construction of a reflectarray system usually begins with a specified gain, which is calculated as the product of the aperture directivity and the aperture efficiency (η_a). The aperture area A determines the aperture directivity through the well-known equation:

$$\text{Directivity} = \frac{4\pi A}{\lambda^2}. \tag{1}$$

Thus, the reflectarray antenna gain is:

$$G = \frac{4\pi A}{\lambda^2}\eta_a. \tag{2}$$

Among many kinds of efficiency factors considered in conventional reflector designs [4, 5], two major terms are studied in this article for reflectarray design: the spillover efficiency (η_s) and the illumination efficiency (η_i). The aperture efficiency is defined as their product:

$$\eta_a = \eta_s\eta_i. \tag{3}$$

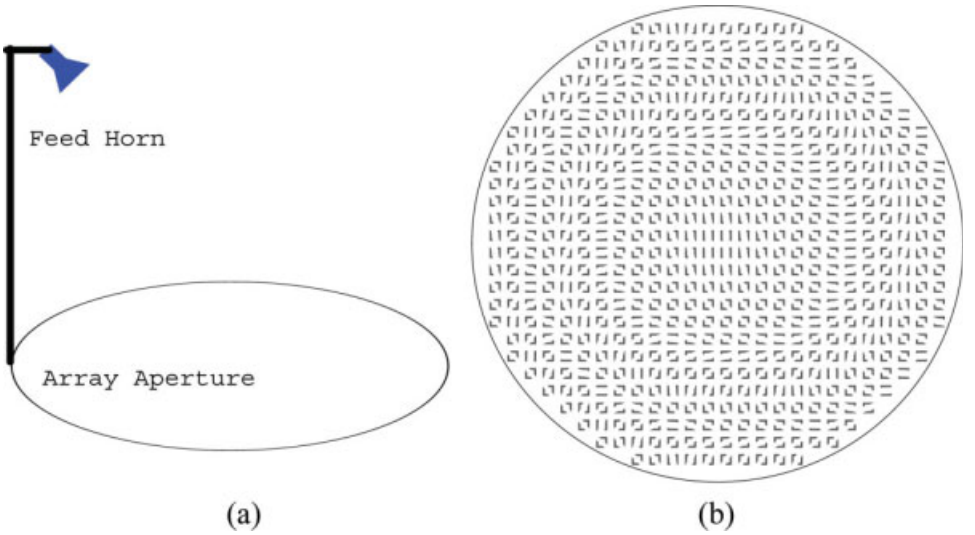

Figure 1 A reflectarray system: (a) general configuration and (b) an example of the array plane. [Color figure can be viewed in the online issue, which is available at www.interscience.wiley.com]

Note that the aperture efficiency discussed here does not include the efficiency factors associated with the feed loss, reflectarray element loss, polarization loss, and mismatch loss.

For conventional parabolic reflector antennas, the relationship between the efficiency and the antenna configuration parameters has been well developed [4, 5]. In this article, a general reflectarray system characterized by a group of configuration parameters will be investigated. A comprehensive derivation will be presented on how the efficiencies are determined, and they are affected by the configuration parameters. It is worthwhile to point out that the general approach presented in this article is applicable in arbitrary reflectarray configurations, including center and offset feed, circular and elliptical aperture.

2. REFLECTARRAY CONFIGURATION PARAMETERS

2.1. Rectangular Coordinates and Feed/Element Patterns

Figure 2 illustrates a rectangular coordinates system established for reflectarray analysis. The origin of the coordinate system (C) is located at the center of the aperture, and the x and y axes are set on the aperture plane. For example, a circular reflectarray aperture with a diameter D is shown in this illustration. The aperture plane is illuminated by a feed source located at F with a projection point F' on the y axis. Therefore, the feed coordinates are F $(0, -H \tan\theta, H)$, where H is the height of the feed and θ_0 is the offset angle.

Various radiation models have been developed to simulate the radiation properties of the feed horn and scattering elements [6]. In this article, the $\cos^q$ pattern is adopted because of its simplicity. In the source region, the feeding beam is assumed to have a normalized power pattern as follows:

$$U_f(\theta,\phi) = \begin{cases} \cos^{2q}\theta & \left(0 \le \theta \le \frac{\pi}{2}\right) \\ 0 & \text{elsewhere} \end{cases} \tag{4}$$

The directivity of the feed antenna and the shape of the pattern are determined by a single parameter q. For example, Figure 3(a) shows the directivity versus the q value, while Figure 3(b) presents several feed antenna patterns at different q values. Basically, the larger the q value, the higher the directivity, and the narrower the antenna beam. The beam direction of the feed antenna is indicated by a point on the array plane, $P_0(x_0, y_0, 0)$, toward which the maximum radiation of the feed horn is pointing.

Next, we model the radiation pattern of a scattering element located at $P(x, y, 0)$. To receive the incident energy, its normalized power pattern is similarly modeled by:

$$U_e(\theta,\phi) = \begin{cases} \cos^{2q_e}\theta_e & \left(0 \le \theta \le \frac{\pi}{2}\right) \\ 0 & \text{elsewhere} \end{cases} \tag{5}$$

Usually, the feed pattern has a larger q value such as 6 and the element pattern has a smaller q_e value such as 1. At the point P, θ is the angle between FP and FP_0, while θ_e is the angle between FP and the normal direction of the aperture plane, as illustrated in Figure 2.

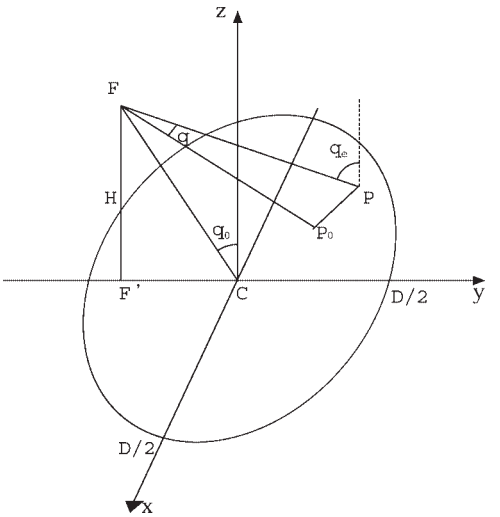

Figure 2 The coordinate system and configuration parameters of a typical reflectarray

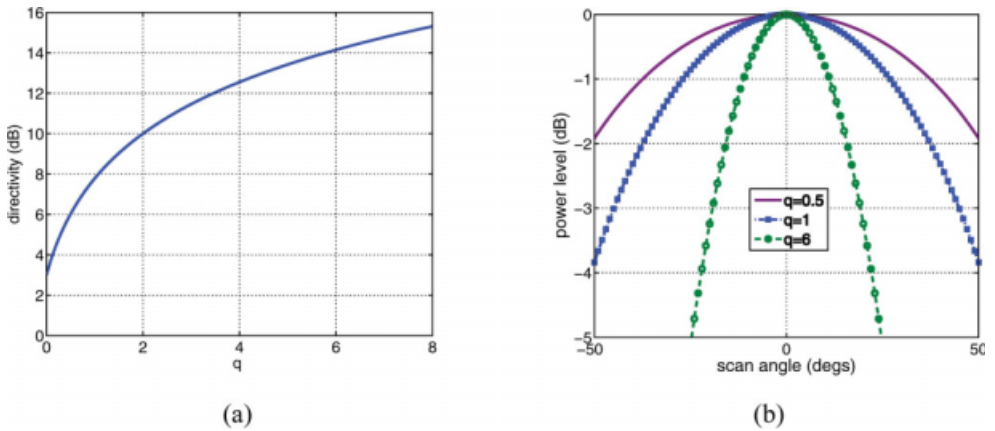

Figure 3 (a) The directivity of a $\cos^q\theta$ pattern, and (b) the power patterns with different q values. [Color figure can be viewed in the online issue, which is available at www.interscience.wiley.com]

2.2. Summary of Reflectarray Parameters and Key Notations

As a brief summary, the aperture efficiency is fully determined by the following reflectarray parameters:

1. The shape and dimensions of the aperture. For a circular aperture, the configuration parameter is the diameter D.
2. The position of the feed, which is characterized by the offset angle θ_0 and the height H.
3. The direction of the feeding beam, which is determined by the point $P_0(x_0, y_0, 0)$.
4. The pattern of the feed with a parameter q.
5. The pattern of the elements with a parameter q_e.

These configuration parameters are labeled in Figure 2. To facilitate the derivation and analysis, all the important geometric quantities involved are listed in Table 1 below.

3. A GENERAL APPROACH TO DETERMINE THE SPILLOVER EFFICIENCY

3.1. Definition

The term "spillover" is defined in Ref. [7], and the spillover efficiency for conventional reflectors is defined in Ref. [4, 5]. Similarly, for reflectarrays, η_s is defined as the percentage of the radiated power from the feed that is intercepted by the reflecting aperture. As illustrated in Figure 4, the evaluation of η_s is thus through the following equation:

$$\eta_s = \frac{\int_\sigma \int \vec{P}(\vec{r})\vec{s}}{\int_\Sigma \int \vec{P}(\vec{r})\vec{s}}, \tag{6}$$

where the denominator is the total power radiated by the feed, and the numerator is the portion of the power incident on the array aperture.

TABLE 1 Important Geometric Quantities in a Reflectarray System

Quantity	Formula
Feed location	$F(0, -H\tan\theta_0, H$
Feed beam point (FBP)	$P_0(x, y_0, 0)$
Element location	$P(x, y, 0)$
Position vector from feed to FBP	$\vec{r}_0 = \overrightarrow{FP}_0 = x_0\hat{x} + (y_0 + H\tan\theta_0)\hat{y} + (-H)\hat{z}$
Distance between the feed and FBP	$r_0 = \lvert FP_0\rvert = \sqrt{x_0^2 + y_0^2 + H^2\sec^2\theta_0 + (2H\tan\theta_0)y_0}$
Position vector from feed to the element	$\vec{r} = \overrightarrow{FP} = x\hat{x} + (y + H\tan\theta_0)\hat{y} + (-H)\hat{z}$
Distance between the feed and the element	$r = \lvert FP\rvert = \sqrt{x^2 + y^2 + H^2\sec^2\theta_0 + (2H\tan\theta_0)y}$
Unit vector from feed to the element	$\hat{r} = \frac{\vec{r}}{r} = \frac{x\hat{x} + (y + H\tan\theta_0)\hat{y} + (-H)\hat{z}}{\sqrt{x^2 + y^2 + H^2\sec^2\theta_0 + (2H\tan\theta_0)y}}$
Distance between element and FBP	$s = \lvert PP_0\rvert = \sqrt{(x - x_0)^2 + (y - y_0)^2}$
Feed pattern parameter	$\cos\theta = \frac{r_0^2 + r^2 - s^2}{2r_0 r}$
Element pattern parameter	$\cos\theta_p = \frac{H}{r}$

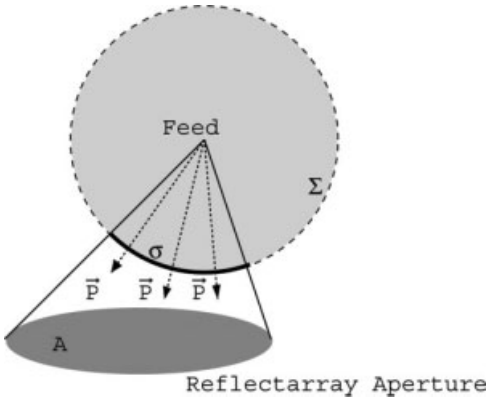

Figure 4 Reflectarray geometry for spillover efficiency analysis

Both integrals are the fluxes of the Poynting vector $\vec{P}(\vec{r})$ through some certain surface areas. Usually, the integral of the denominator is performed over the entire spherical surface centered at the feed, denoted by Σ. This integral can be evaluated either numerically or analytically, given a proper form of $\vec{P}(\vec{r})$. The integral in the numerator is evaluated over a portion σ of the sphere, where σ and the array aperture share the same solid angle with respect to the feed. The procedure to compute η_s using Eq. (17) is called the direct approach.

Practically, only the dimensions of the aperture are known, hence it is necessary to determine the boundary of σ in terms of the spherical coordinates of the feed. For special cases such as a circular array aperture with a center feed, the boundary of σ can be determined easily. However, in general cases, for instance, an offset feed case or a square shaped aperture, it is not so straightforward to determine the boundary of σ. Thus, it is difficult to calculate the integral in the numerator using the direct approach.

An alternative approach is proposed here to solve this problem, by performing the integral over the array aperture A instead of on the surface σ of the sphere,

$$\eta_s = \frac{\int_A \int \vec{P}(\vec{r}) \cdot d\vec{s}}{\int_\Sigma \int \vec{P}(\vec{r}) \cdot d\vec{s}}. \tag{7}$$

The approach is general and straightforward because the integral in the numerator is calculated in a coordinate system that accommodates the shape of the array boundary. Moreover, the flexibility is introduced to have an arbitrary position of the feed.

3.2. Calculation of the Spillover Efficiency

The Poynting vector of the feed defined by the power pattern Eq. (4) can be written in terms of the source region spherical coordinates as:

$$\vec{P}(\vec{r}) = \hat{r}\frac{\cos^{2q}\theta}{r^2}\left(0 \le \theta \le \frac{\pi}{2}\right). \tag{8}$$

Hence the denominator in Eq. (6) can be determined analytically:

$$I_d = \int_0^{2\pi}\int_0^{\pi/2} \cos^{2q}\theta \sin\theta \sin\theta \, d\theta d\phi = \frac{2\pi}{2q+1}. \tag{9}$$

The integral in the numerator of Eq. (6) is replaced by:

$$I_n = \iint_A \vec{P}(\vec{r}) \cdot d\vec{s}, \tag{10}$$

where the integration is performed over the array aperture A. The physical explanation is that the array aperture and the spherical surface portion σ have the same solid angle with respect to the feed. To calculate Eq. (10), the Poynting vector in Eq. (8) should be rewritten in the rectangular coordinates, as shown in Figure 2. For an arbitrary point $P(x, y, 0)$ on the array aperture, using the configuration parameters in Table 1, it is obtained that:

$$\vec{P}(\vec{r}) = \frac{1}{r^3}\left(\frac{r_0^2 + r^2 - s^2}{2r_0 r}\right)^{2q}[x\hat{x} + (y + H\tan\theta_0)\hat{y} + (-H)\hat{z}]. \tag{11}$$

Hence in Eq. (10), the integrand has the following expression:

$$\vec{P}(\vec{r}) \cdot d\vec{s} = \frac{H}{r^3}\left(\frac{r_0^2 + r^2 - s^2}{2r_0 r}\right)^{2q} dxdy. \tag{12}$$

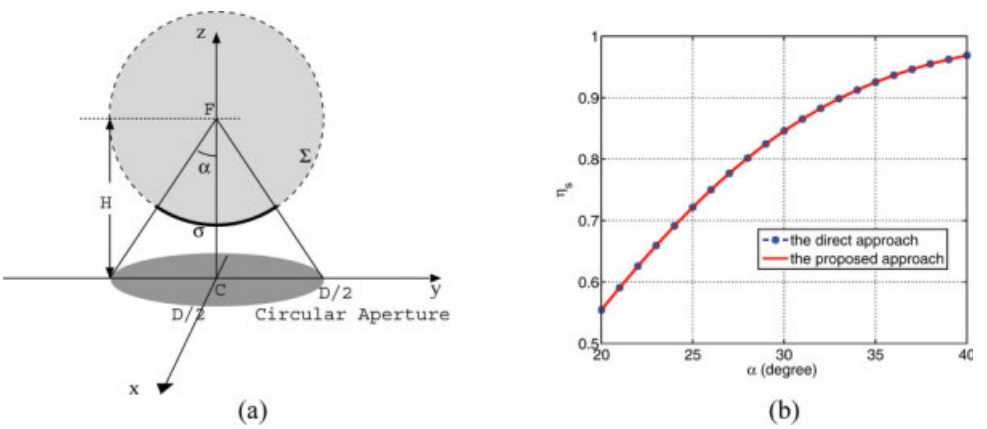

Figure 5 A center-feed circular-aperture reflectarray: (a) antenna configuration and (b) the spillover efficiency result compared with that of the direct approach. [Color figure can be viewed in the online issue, which is available at www.interscience.wiley.com]

TABLE 2 Configuration Parameters of the Two Special Reflectarray Cases

Case	θ_0	H	q	x_0	y_0
1	0°	340 mm	6	0	0
2	25°	340 mm	6	0	0

Note that the differential surface element has a $-z$ normal direction. Then, the integral Eq. (10) can be evaluated numerically for general array apertures. When the array aperture has a circular shape, one can also use the polar coordinates for the surface integration as follows,

$$I_n = \int_0^{2\pi}\int_0^{D/2} \frac{H}{r^3}\left(\frac{r_0^2 + r^2 - s^2}{2r_0 r}\right)^{2q} \rho \mathrm{d}\rho \mathrm{d}\varphi. \tag{13}$$

Finally, the spillover efficiency is obtained as:

$$\eta_s = \frac{I_n}{I_d} = \frac{2q+1}{2\pi}\int_0^{2\pi}\int_0^{D/2} \frac{H}{r^3}\left(\frac{r_0^2 + r^2 - s^2}{2r_0 r}\right)^{2q} \rho \mathrm{d}\rho \mathrm{d}\varphi. \tag{14}$$

In summary, η_s is a function of six reflectarray parameters:

$$\eta_s = \eta_s(D, \theta_0, H, q, x_0, y_0). \tag{15}$$

It is noted that among all the configuration parameters summarized in Section 2.2, the spillover efficiency is only independent from the element pattern parameter q_e.

3.3. Verification of the Proposed Approach

To verify the proposed approach, two special cases are considered, where the surface σ is a simple conical surface, and the integral can be calculated analytically. The first example is a central feed reflectarray with a circular aperture, as shown in Figure 5(a). The system configuration parameters are listed in Table 2. Since the offset angle θ_0 is zero and the feed beam is pointing to the center of the reflectarray aperture, the geometrical quantities in Table 1 is simplified and rewritten in Table 3.

For this case, the integral in the numerator of Eq. (6) can also be evaluated directly over σ under the pattern model Eq. (4). The analytical result is:

$$\iint_\sigma \vec{P}(\vec{r})\cdot d\vec{s} = \int_0^{2\pi}\int_0^{\alpha} \cos^{2q}\theta \sin\theta \, d\theta d\phi = \frac{2\pi}{2q+1}(1 - \cos^{2q+1}\alpha), \tag{16}$$

where the angle α is introduced as a variable representing the half aperture angle of the cone. Equations (9) and (16) lead to:

$$\eta_s = 1 - \cos^{2q+1}\alpha. \tag{17}$$

The comparison between numerical integration and analytical result is shown in Figure 5(b). Since H is fixed, the diameter of the reflectarray is varying with α. The spillover efficiency increases as the angle α grows. The analytical and numerical results agree very well with each other.

The second case is illustrated in Figure 6(a), with an offset feed. Suppose the array aperture subtends the same solid angle about the feed as the first case. Hence the same σ is considered and the same spillover efficiency as Eq. (17) is obtained. However, the array plane is not perpendicularly intercepting the beam; instead, it is cutting the conical region obliquely. As is known, this results in an elliptical shape of the array aperture. The boundary equation reads:

$$x^2 + (y\cos\theta_0)^2 = (y\sin\theta_0 + H/\cos\theta_0)^2 \tan^2\alpha. \tag{18}$$

The system configuration parameters are also listed in Table 2. The numerical integration procedure follows the general approach introduced in Section 3.2. In particular, the integration is restricted in the inner area of the ellipse defined by Eq. (18). Again, α is varied when comparing the analytical and numerical results, as demonstrated in Figure 6(b). Good agreement is again achieved for this example. This case also demonstrates that the proposed approach is able to deal with an arbitrary shape of the aperture, because the numerical integration can be performed within any specified planar boundary.

4. COMPUTATION OF THE ILLUMINATION EFFICIENCY

The definition of the illumination efficiency can be extended from that of the conventional reflector antennas [4, 5] to reflectarrays.

$$\eta_i = \frac{1}{A_a}\frac{\left|\iint_A I(x,y)dA\right|^2}{\iint_A |I(x,y)|^2 dA}, \tag{19}$$

where $I(x,y)$ is the amplitude distribution over the aperture. Here it is assumed that the field is purely in a certain polarization. In this definition, the amplitude $I(x,y)$ relies on the patterns of both the feed and the reflectarray element. Using the pattern models (4) and (5), it is obtained for the configuration in Figure 2 that:

TABLE 3 Important Geometric Quantities for a Central Feed Circular Reflectarray System

Quantity	Formula
Feed location	$F(0, 0, H)$
Feed beam point (FBP)	$P_0(x_0, y_0, 0)$
Element location	$P_0(x, y, 0)$
Position vector from feed to FBP	$\vec{r}_0 = \overrightarrow{FP}_0 = x_0\hat{x} + y_0\hat{y} + (-H)\hat{z}$
Distance between the feed and FBP	$r_0 = \lvert FP_0\rvert = \sqrt{x_0^2 + y_0^2 + H^2}$
Position vector from feed to the element	$\vec{r} = \overrightarrow{FP} = x\hat{x} + y\hat{y} + (-H)\hat{z}$
Distance between the feed and the element	$r = \lvert FP\rvert = \sqrt{x^2 + y^2 + H^2}$
Unit vector from feed to the element	$\hat{r} = \frac{\vec{r}}{r} = \frac{x\hat{x} + y\hat{y} + (-H)\hat{z}}{\sqrt{x^2 + y^2 + H^2}}$
Distance between element and FBP	$s = \lvert PP_0\rvert = \sqrt{(x - x_0)^2 + (y - y_0)^2}$
Feed pattern parameter	$\cos\theta = \frac{r_0^2 + r^2 - s^2}{2r_0 r}$
Element pattern parameter	$\cos\theta_p = \frac{H}{r}$

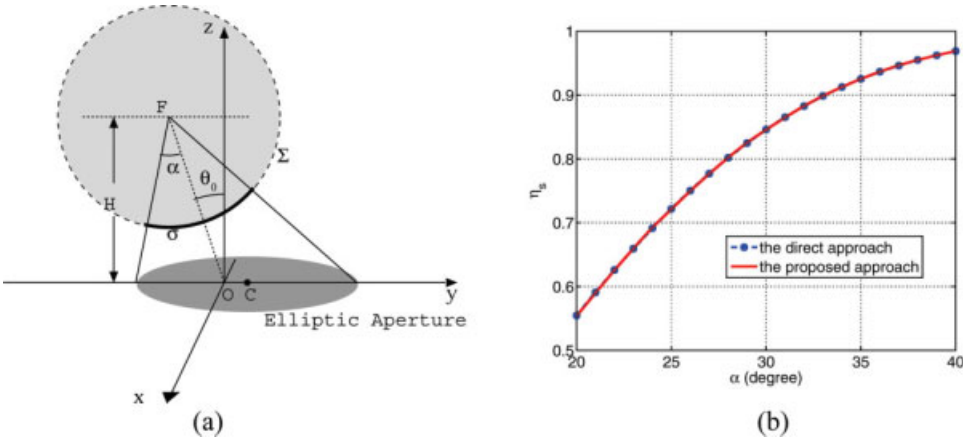

Figure 6 An offset-feed elliptical-aperture reflectarray antenna: (a) antenna configuration and (b) the spillover efficiency result compared with that of the direct approach. [Color figure can be viewed in the online issue, which is available at www.interscience.wiley.com]

$$I(x,y) \propto \frac{\cos^q \theta \cos^{q_e} \theta_p}{r}, \tag{20}$$

where the denominator r is introduced due to the path length during the wave propagation. Therefore, by applying the same geometric quantities derived in Section 2, it is obtained that:

$$I(x,y) = \frac{1}{r}\left(\frac{r_0^2 + r^2 - s^2}{2r_0 r}\right)^q \left(\frac{H}{r}\right)^{q_e} = \frac{H^{q_e}}{r^{1+q_e}}\left(\frac{r_0^2 + r^2 - s^2}{2r_0 r}\right)^q. \tag{20}$$

For a circular aperture, it is convenient to have an integral form in polar coordinates:

$$\eta_i = \frac{4}{\pi D^2}\frac{\left[\int_0^{2\pi}\int_0^{D/2} \frac{1}{r^{1+q_e}}\left(\frac{r_0^2+r^2-s^2}{2r_0 r}\right)^q \rho \mathrm{d}\rho \mathrm{d}\varphi\right]^2}{\int_0^{2\pi}\int_0^{D/2} \frac{1}{r^{2+2q_e}}\left(\frac{r_0^2+r^2-s^2}{2r_0 r}\right)^{2q} \rho \mathrm{d}\rho \mathrm{d}\varphi}. \tag{21}$$

This result shows that η_i is a function of seven parameters:

$$\eta_i = \eta_i(D, \theta_0, H, q, x_0, y_0, q_e). \tag{22}$$

In Figure 3(a) it is observed that when $q_e = 1$ the directivity is about 7.78 dB. This directivity is close to that of a microstrip patch conventionally applied as the scattering element in reflectarray designs. Hence this value of q_e is assumed in the following reflectarray analysis.

5. PARAMETRIC STUDIES ON THE REFLECTARRAY APERTURE EFFICIENCY

Once the spillover efficiency and illumination efficiency are determined from Eqs. (15) and (22), the reflectarray aperture efficiency is calculated as follows:

$$\eta_a = \eta_s \eta_i = \eta_a(D, \theta_0, H, q, x_0, y_0, q_e). \tag{23}$$

In practical reflectarray designs, it is desired to search for the maximum aperture efficiency in a given parameter space and identify the corresponding configuration parameters. To achieve this goal, it is necessary to obtain some qualitative insights on how the reflectarray parameters are associated with the aperture efficiency.

The reflectarray configuration parameters figured out in Section 2 have been categorized into five groups. The first parameter D is usually determined by a chosen directivity in accordance with Eq. (1). Hence it is set at a fixed value (here 500 mm) in the following parametric study. The effects of other four groups of parameters are presented one by one.

5.1. Feed Location

The feed position is characterized by two geometric parameters: the offset angle θ_0 and the height H, as demonstrated in Figure 2. If the other parameters in Eq. (23) are fixed, it is obtained that:

$$\eta_a = \eta_a(\theta_0, H) \tag{24}$$

The effects of θ_0 and H are studied individually as shown in Figures 7(a) and 7(b) with the other reflectarray parameters set as: $q = 6$, $x_0 = 0$, $y_0 = 0$, $q_e = 1$.

As θ_0 varies, the results from Eqs. (15), (22), and (23) are demonstrated in Figure 7(a), where the feed height $H = 340$ mm. When θ_0 increases, the spillover efficiency decreases but the illumination efficiency increases. As their product, the maximum aperture efficiency appears at the central feed case ($\theta_0 = 0$) and remains similar in a certain range of the offset angle θ_0. In some applications, people would like to use offset feed to minimize the feed blockage loss. As revealed here, the aperture efficiency for the offset feed case maintains almost constant until θ_0 is up to 20°. Even at an offset angle of 30°, the efficiency only drops from 75 to 73%.

On the other hand, Figure 7(b) shows the aperture efficiencies versus the feed height H. In this study, the offset angle θ_0 is set at 25°. As H grows, the spillover efficiency decreases, since a larger height leads to a reduced aperture angle of the reflectarray plane with respect to the feed source. Meanwhile the illumination efficiency increases due to a more uniform field distribution on the array. The aperture efficiency reaches a maximum when H/D is equal to 0.71 in this example. It is calculated

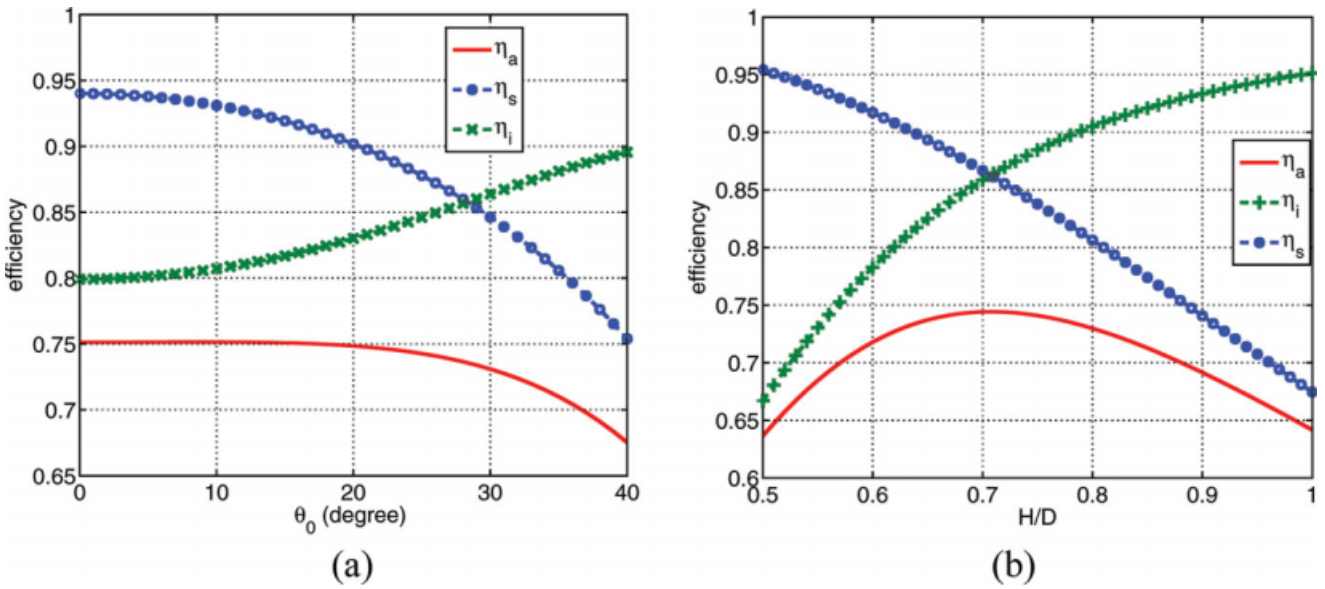

Figure 7 Efficiencies vs. (a) θ_0 and (b) H (normalized to aperture diameter). [Color figure can be viewed in the online issue, which is available at www.interscience.wiley.com]

that edge taper in this setup is around −9 dB, which is similar to traditional reflector antennas.

Since the feed is located in the yz plane (the plane of incidence), it is convenient to use the coordinate (y_f, z_f) derived from θ_0 and H:

$$\begin{cases} y_f = -H\tan\theta_0 \\ z_f = H \end{cases} \tag{25}$$

Thus, Eq. (24) is rewritten as:

$$\eta_a = \eta_a(y, z) \tag{26}$$

This allows a contoured view of the efficiency variation associated to the feed location in the plane of incidence. The results are demonstrated in Figures 8(a) and 8(b) for $q = 6$ and $q = 8$, respectively. It is noted that when $q = 6$, the total aperture efficiency is varying slowly from 66 to 77%. When $q = 8$, the maximum aperture efficiency is achieved at a higher feed position. The reason is that, with a narrower feeding beam the illumination efficiency cannot be improved if the source is too close to the array plane. Using this contour map, one can feel confident to select a proper feed location. Another phenomenon worthy of noting is that when $q = 8$, at a moderate height around 340 mm, an offset feed can result in a slightly larger aperture efficiency than the central feed. This is observed from the special shape of the contour in Figure 8(b).

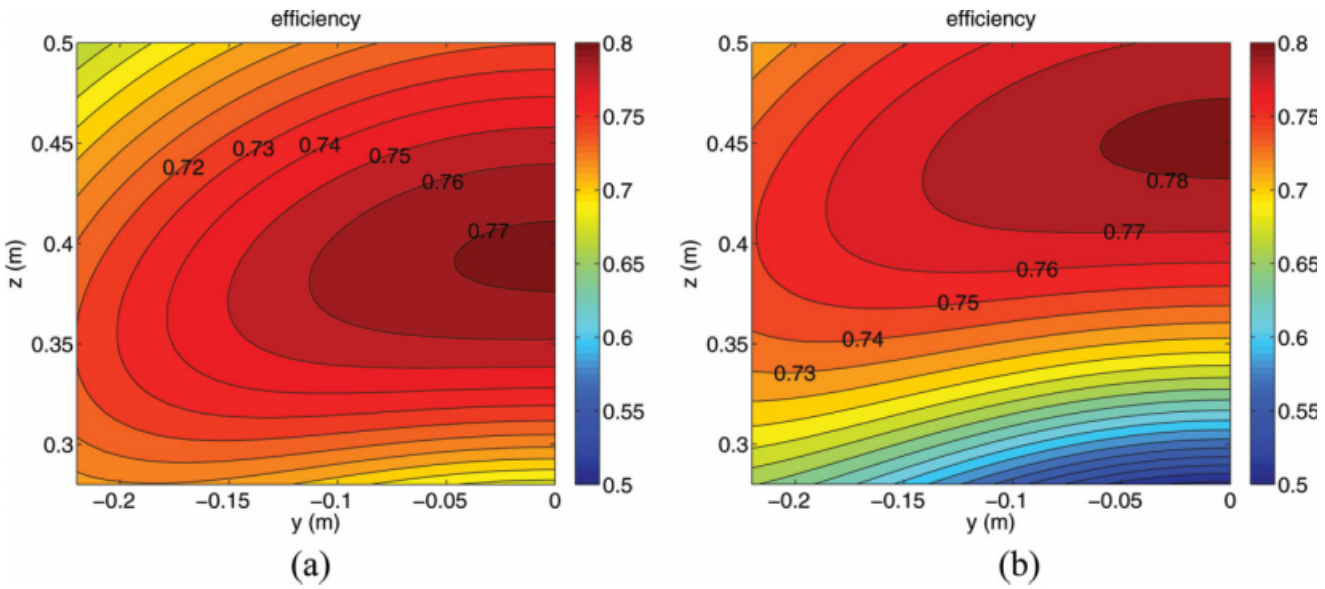

Figure 8 Total aperture efficiency vs. the feed location (y,z) in the plane of incidence with (a) $q = 6$ and (b) $q = 8$. [Color figure can be viewed in the online issue, which is available at www.interscience.wiley.com]

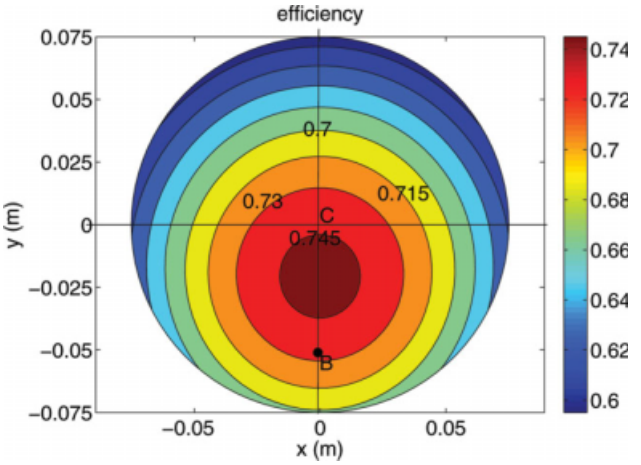

Figure 9 Total aperture efficiency vs. feed orientation $P_0(x_0, y_0, 0)$. [Color figure can be viewed in the online issue, which is available at www.interscience.wiley.com]

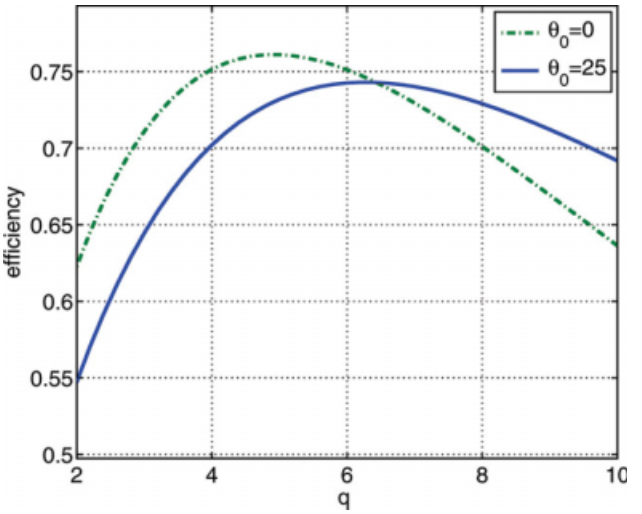

Figure 10 Total aperture efficiency vs. q. [Color figure can be viewed in the online issue, which is available at www.interscience.wiley.com]

5.2. *Feed Orientation*

The feed orientation is described by two geometric parameters: x_0 and y_0, the coordinates of the point P_0. By fixing the other parameters, the total aperture efficiency is reduced to:

$$\eta_a = \eta_a(x_0, y_0) \tag{27}$$

Using the fixed parameters: $\theta_0 = 25°$, $H = 340$ mm, $q = 6$, and $q_e = 1$, the contoured aperture efficiency plot is shown in Figure 9. On this plot, it is interesting to observe the aperture efficiency η_a at two special cases. One is with the feeding beam pointing toward the array center point, whereas the other is the bi-sect point of the aperture angle subtended by the diameter. These two points are marked by C, where $\eta_a = 74.1\%$, and B, where $\eta_a = 73.4\%$. The distance between the bi-sect point B and the center point C is 51 mm. It is noted that the maximum efficiency is obtained when the feeding beam is pointing at an intermediate point that is about 20 mm away from the array center, where η_a reaches 74.8%. This optimum point is also the result of a compromise between the spillover efficiency and the illumination efficiency, since the former is higher at point B to have most of the energy intercepted, whereas the latter prefers point C so that a more uniform field distribution is achieved.

5.3. *Feed Pattern*

The feed pattern is modeled using a single parameter q, as previously shown in Eq. (4). The feed pattern may also be the subreflector pattern in a Cassegrain configuration. The total aperture efficiency will reduce to:

$$\eta_a = \eta_a(q) \tag{28}$$

when the other parameters are constant. The curve of this function is depicted in Figure 10, where it is assumed that $H = 340$ mm, $x_0 = 0$, $y_0 = 0$, and $q_e = 1$. Again the opposite tendencies of η_s and η_i lead to an optimum value of q where the total aperture efficiency is maximized. For example, the optimum q is 4.9 for the central feed case and 6.3 for 25°, the offset feed case. It is observed that when using a central feed, a smaller q value, hence a wider feeding beam is preferred to have the maximum aperture efficiency. This indicates that the illumination efficiency is a more dominant factor, since the wider the beam, the more uniform the field distribution is.

5.4. *Element Pattern*

The element pattern is modeled using a single parameter q_e, as previously shown in Eq. (5). Similarly, the curve of the following aperture efficiency expression is plot in Figure 11:

$$\eta_a = \eta_a(q_e), \tag{29}$$

where $H = 340$ mm, $x_0 = 0$, $y_0 = 0$, and $q = 6$. Note that the parameter q_e only affects η_s. A larger q_e weighted on the illumination increases the nonuniformity; hence the total efficiency is monotonically decreasing. Consideration of both the feed and the array element patterns leads to a contour plot of the aperture efficiency in Figure 12, showing the fact that the element

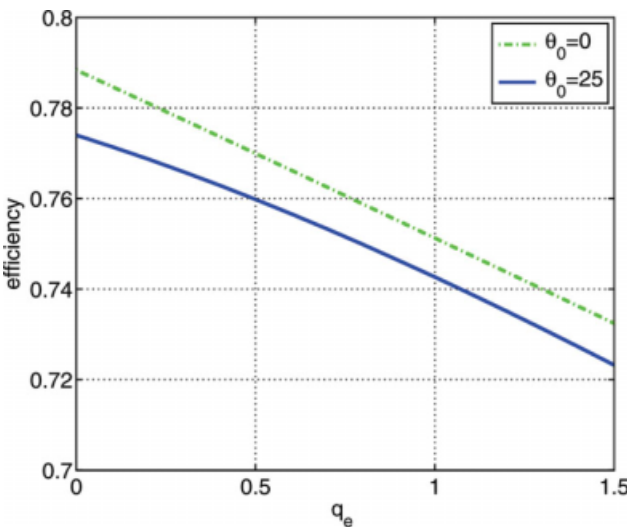

Figure 11 Total aperture efficiency vs. q_e. [Color figure can be viewed in the online issue, which is available at www.interscience.wiley.com]

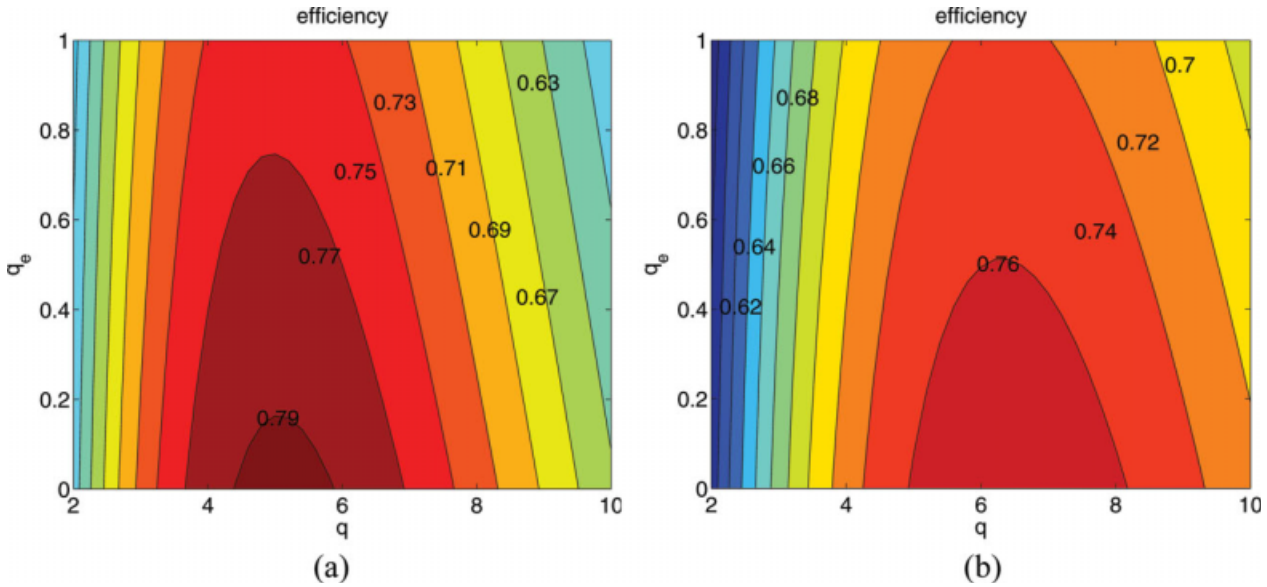

Figure 12 Total aperture efficiency vs. both q and q_e under (a) central feed and (b) offset feed. [Color figure can be viewed in the online issue, which is available at www.interscience.wiley.com]

pattern plays a less significant role in the total aperture efficiency than the feed pattern.

5.5. *Summary*

Through earlier parametric studies, we can obtain to the following rules of thumb to start the design of a reflectarray:

1. The feed location plays an important role to determine the aperture efficiency of the reflectarray. Generally, a central feed ($\theta_0 = 0$) has the maximum aperture efficiency. The feed height varies with the beam width of the feeding source. A narrower beam needs a larger height. For example, when $q = 6$, the optimum height is around 0.8 D, while a height of 0.9 D is the best for $q = 8$. The edge tapers are -8.6 and -9.3 dB, respectively in these cases, which is close to traditional reflector antennas.
2. The offset feed reflectarray has smaller aperture efficiency; however, the degradation is trivial when the offset angle is in a certain range. For example, the efficiency only drops from 75 to 73% for up to 30° offset angle. In addition, at some specific heights and q values of the horn, an offset feed can achieve higher aperture efficiency than the central feed at the same height. Furthermore, the maximum efficiency of an offset case is usually obtained when the feeding beam is directed to a point between the aperture center and the bisect point of the aperture angle.
3. The feeding beam needs to be moderately directive, with q in a range between 4 and 8 using a $\cos^q\theta$ pattern model. Meanwhile, the pattern of the reflectarray element is not quite critical under this condition.

6. CONCLUSION

The estimation of the total aperture efficiency is necessary in reflectarray designs. This article summarizes a group of configuration parameters of a reflectarray system that are associated with the aperture efficiency. A general approach is proposed to compute the spillover efficiency, which can be applied to any aperture shape and any feed position. The aperture efficiency of the reflectarray is obtained when the illumination efficiency is also determined using the unified set of equations. A parametric study is performed thereafter, in which the effects of the configuration parameters are analyzed and some engineering guidance on feed location, feed beam direction, feed pattern, and element pattern are obtained to maximize the aperture efficiency of reflectarray antennas.

REFERENCES

1. D.G. Berry, R.G. Malech, and W.A. Kennedy, The reflectarray antenna, IEEE Trans Antennas Propag 11 (1963), 645–651.
2. J. Huang and J.A. Encinar, Reflectarray antennas, IEEE-Wiley, Hoboken, NJ, 2007.
3. D.M. Pozar, S.D. Targonski, and H.D. Syrigos, Design of millimeter wave microstrip reflectarray, IEEE Trans Antennas Propag 45 (1997), 287–296.
4. A.W. Rudge, K. Milne, A.D. Olver, and P. Knight, The handbook of antenna design, Vol. 1 and 2, Chapter 3, 1986, pp. 169–182.
5. Y. Rahmat-Samii, Reflector antenna analysis, synthesis and measurements: Modern topics, Lecture notes, Electrical Engineering Department, University of California at Los Angeles, 2003.
6. T. Milligan, Modern antenna design, 2nd ed., John Wiley, Hoboken, NJ, 2005.
7. IEEE Standard #145, Definitions of terms for antennas, IEEE Trans Antennas Propag 17 (1969), 262–269.